Importance Weighting for Aligning Language Models under Deployment Distribution Shift

Anonymous authors
Paper under double-blind review

Abstract

Aligning language models (LMs) with human preferences remains challenging partly because popular approaches, such as reinforcement learning from human feedback and direct preference optimization (DPO), often assume that the training data is sufficiently representative of the environment in which the model will be deployed. However, real-world applications frequently involve distribution shifts, e.g., changes in end-user behavior or preferences during usage or deployment, which pose a significant challenge to LM alignment approaches. In this paper, we propose an importance weighting method tailored for DPO, namely IW-DPO, to address distribution shifts in LM alignment. IW-DPO can be applied to joint distribution shifts in the prompts, responses, and preference labels without explicitly assuming the type of distribution shift. Our experimental results on various distribution shift scenarios demonstrate the usefulness of IW-DPO.

1 Introduction

While language models (LMs) have been rapidly increasing their language generation capabilities in recent years, aligning them with human values and norms remains a challenging task (Shen et al., 2023). Among the various approaches for alignment, reinforcement learning from human feedback (RLHF) has demonstrated considerable success in aligning LMs with human preferences (Ziegler et al., 2019; Stiennon et al., 2020; Ouyang et al., 2022). However, it is involved in a rather complex training pipeline: reward modeling (RM) from preference data and optimization of an LM using a learned reward model and a reinforcement learning (RL) algorithm. To reduce this complexity, Rafailov et al. (2024) developed a simple yet effective optimization approach, namely direct preference optimization (DPO). DPO directly optimizes the LM without the need for RM and RL, thus making it simpler and faster.

DPO has been demonstrated to be an effective method for fine-tuning LMs to generate responses that align with human-desired outputs, leading to the creation of several widely used foundation LM families, such as Llama 3 (Grattafiori et al., 2024), Phi-4 (Abdin et al., 2024), Qwen2 (Yang et al., 2024), and DeepSeek (Bi et al., 2024). Like other machine learning algorithms (Quiñonero-Candela et al., 2008; Pan & Yang, 2009; Sugiyama & Kawanabe, 2012), however, DPO typically suffers from various distribution shifts that present a challenge in aligning with human-desired responses, underscoring the need for the development of a method that can effectively address such practical difficulties.

Recent studies have attempted to address the issue of distribution shifts in DPO, where the LM being optimized gradually deviates from the initial reference model (the LM used as initial weights for training) as training progresses on a fixed offline preference dataset, which we refer to as *model distribution shift*. For instance, Sun et al. (2023) proposed a way to address the difference between the reward distribution of the LM and that of the reference model. Gou & Nguyen (2024), Zhou et al. (2024) and Xu et al. (2024) explored a phenomenon in which the output (also called sample, response or completion in various literature) distribution of the LM changes, causing it to diverge from the distribution present in the fixed offline preference dataset. Similarly, Dou et al. (2024) examined how output distribution shifts negatively impact the performance of the reward model, diminishing its ability to distinguish between responses.

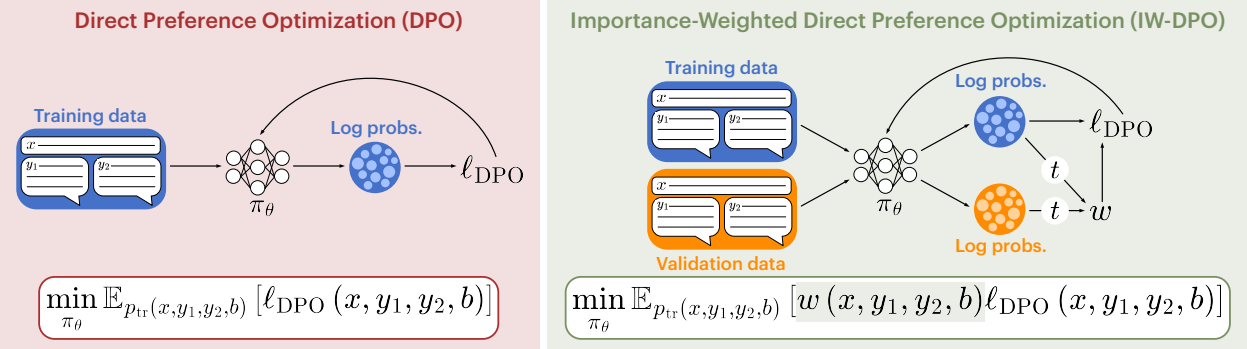

Figure 1: DPO optimizes for the training distribution by using only the training data, while **IW-DPO optimizes for the test distribution by additionally using a tiny amount of data (i.e., validation data) sampled from the test distribution to estimate weights and reweight training losses.** In weight estimation, the log probabilities of the training data and those of the validation data are passed through a transformation function t, and the transformed data are then used to compute the importance weights.

In contrast, our work addresses a fundamentally different form of distribution shift which we call the *deployment distribution shift*, where the environment changes in ways not reflected in the training dataset. Such shifts can arise from real-world usage or deployment, such as changes in end-user behavior or preferences. For the remainder of this paper, we will use the term "distribution shift" to denote this phenomenon. We characterize the factors that cause distribution shifts in LM alignment and, accordingly, systematically define the types of distribution shifts. Specifically, in the context of LM alignment, preference data typically consists of three elements: prompt, response, and preference label. Various types of distribution shifts between the training distribution and post-deployment, i.e., the test distribution, can arise from one or more of these factors. When a distribution shift occurs, training on the training dataset means optimizing for the training distribution, which may result in poor performance on the test distribution. Son et al. (2024) explored a shift in one of these factors, the preference shift problem, but focused on an online setting, whereas we assume to have a fixed offline preference dataset for training. We provide a detailed explanation of the definition of distribution shift, the contributing factors, and the types of distribution shifts in Section 3.1.

For solving distribution shift problems, importance weighting is a powerful tool that estimates a test-over-training density ratio as weights and uses these weights to reweight the training losses (Sugiyama & Kawanabe, 2012). Later, dynamic importance weighting (DIW) was proposed as a modern implementation of importance weighting, which makes it well suited for deep learning (Fang et al., 2020). However, DIW mainly focuses on classification, and its effectiveness in large-scale machine learning problems such as LM alignment has yet to be investigated.

In this paper, inspired by DIW, we propose an importance-weighted DPO, namely IW-DPO, to solve the distribution shifts in LM alignment. An overview of our method compared to the original DPO is shown in Figure 1. IW-DPO estimates importance weights for training instances and uses them to up/down-weight training instances that are relevant/irrelevant to ensure that the LM is not overfitted to the training distribution and more aligned with the test distribution. To estimate the importance weights, IW-DPO uses a transformation function t derived from the LM to convert raw preference data into low-dimensional representations. It then performs existing density ratio estimation methods, such as kernel mean matching (KMM) (Huang et al., 2006), Kullback–Leibler importance estimation procedure (KLIEP) (Sugiyama et al., 2007) and relative unconstrained least-squares importance fitting (RuLSIF) (Yamada et al., 2011), on the transformed data.

A significant advantage of IW-DPO is its capability to handle joint distribution shifts without requiring prior knowledge of the types of distribution shifts involved, making it particularly valuable for practical applications. To evaluate its effectiveness, we design and conduct experiments under various distribution shift scenarios in LM alignment. The results show a great potential of IW-DPO in handling practical distribution shift problems.

2 Related Work and Background

In this section, we first explore various approaches to importance weighting in LMs and then provide the background information on reward-based and reward-free RLHF.

2.1 Importance Weighting in LMs

Several approaches based on importance weighting have been proposed for language modeling. Grangier et al. (2023) proposed an importance weighting method for LM pre-training and fine-tuning, where importance weights are estimated by a separate weighting model trained jointly with the LM. While they concentrated on LM pre-training and fine-tuning, our emphasis is on LM alignment, particularly preference optimization. Moreover, our IW-DPO utilizes a transformation function from the LM for weight estimation, eliminating the need for joint training of a weighting model as they did. Jiang et al. (2024) applied importance weighting as a form of importance sampling to filter out self-generated examples that deviate from the desired distribution, aiming for self-improvement in LMs. However, their approach is constrained to datasets or tasks with clear, definitive answers because it includes components such as self-consistency and majority voting, whereas our focus is on more open-ended tasks. Zhou et al. (2024) proposed an extension of DPO, namely weighted preference optimization (WPO). Their approach involves reweighting training instances to address the distribution shift between the output distribution of the LM and the distribution presented in the training preference dataset. While WPO focuses on the model distribution shift, we focus on the deployment distribution shift. In addition, while WPO uses length-normalized sequence probabilities (i.e., probabilities of all predicted tokens in the response) as weights, IW-DPO estimates weights by using a density ratio estimation method. Sow et al. (2025) introduced an importance weighting method for LM pre-training with weight estimation based on training losses; however, they did not account for any distribution shifts. Additionally, their weight estimation method computes importance weights solely based on information from the training examples, specifically using training loss values. In contrast, our weight estimation process accounts for using information from both training and test distributions, thereby optimizing specifically for the test distribution.

2.2 RLHF

Reward-based RLHF In reward-based RLHF, following the pipeline in Stiennon et al. (2020), we first construct a reward model that approximates human preferences based on a pair of responses (y_1, y_2) to a given prompt x.[1] Human annotators express a preference for one response over the other, referred to as preference label b, which is used to train the reward model. We define $b = +1$ if y_1 is preferred, and $b = -1$ if y_2 is preferred. One common approach for modeling human preferences is the Bradley-Terry model (Bradley & Terry, 1952), which defines the preference probability expressed as

$$p(b \mid x, y_1, y_2) = \sigma\left(b \cdot \left(r^*(x, y_1) - r^*(x, y_2)\right)\right), \tag{1}$$

where r^* is a latent reward model and $\sigma(u) = \frac{1}{1+\exp(-u)}$ is the sigmoid function. We are given a preference dataset $\mathcal{D} = \{(x^i, y_1^i, y_2^i, b^i)\}_{i=1}^N$ of N instances. During the RM phase, we aim to optimize the following objective to train a reward model r_ψ parameterized by ψ:

$$\min_{r_\psi} \mathbb{E}_{(x,y_1,y_2,b)\sim\mathcal{D}}\left[-\log\sigma\left(b \cdot \left(r_\psi(x, y_1) - r_\psi(x, y_2)\right)\right)\right]. \tag{2}$$

After training the reward model, we proceed to the RL phase where we consider optimizing an LM π_θ parameterized by θ.[2] The goal of this phase is to maximize the expected reward assigned to the generated response of the LM π_θ while ensuring that it does not drift too far from the reference model π_{ref}. This can be done by utilizing proximal policy optimization (Schulman et al., 2017), which results in the following objective:

[1] Some RLHF pipelines, such as those in Ziegler et al. (2019) and Ouyang et al. (2022), may utilize more than two responses.

[2] Given a prompt x, π_θ generates a response y in an auto-regressive manner characterized by $\pi_\theta(y \mid x) = \prod_j \pi_\theta\left(y_j \mid x, y_{<j}\right)$, where y_j is the j-th token in the response and $y_{<j}$ is the tokens in the response prior to y_j (Xu et al., 2024).

$$\max_{\pi_\theta} \mathbb{E}_{x\sim\mathcal{D}_x, y\sim\pi_\theta(y|x)} \left[r_\psi(x,y)\right] - \beta\mathbb{D}_{\mathrm{KL}}\left[\pi_\theta(\cdot \mid x)\|\pi_{\mathrm{ref}}(\cdot \mid x)\right], \tag{3}$$

where y is a response generated by π_θ given a prompt x sampled from $\mathcal{D}_x = \{x^i\}_{i=1}^N$, and $\mathbb{D}_{\mathrm{KL}}$ is the Kullback–Leibler (KL) divergence and ensures that the LM does not diverge too far from the reference model, as controlled by a hyperparameter $\beta > 0$.

Reward-free RLHF DPO (Rafailov et al., 2024) simplifies the RLHF process by directly optimizing the LM using human preference data, without the need for RM and RL. The derivation of the DPO loss begins by reparameterizing the reward function in terms of the LM π_θ and the reference model π_{ref}, resulting in an implicit reward function r. We can then express the probability of human preferences in terms of the LM directly, thereby bypassing the need to fit an explicit reward model (Rafailov et al., 2024). This results in the DPO loss, which is defined as

$$\ell_{\mathrm{DPO}}(x, y_1, y_2, b) = -\log\sigma\left(b\cdot(r(x,y_1) - r(x,y_2))\right), \tag{4}$$

where the implicit reward function r is given by

$$r(x,y) = \beta\log\frac{\pi_\theta(y \mid x)}{\pi_{\mathrm{ref}}(y \mid x)}. \tag{5}$$

Going forward, we will omit x in Eq. (5) for simplicity. In practice, a simple way to derive π_θ and π_{ref} is to initialize them to a supervised fine-tuned LM (Rafailov et al., 2024), which we will refer to as supervised fine-tuning (SFT).[3]

3 Proposed Method

In this section, we introduce the mechanism of IW-DPO. We begin by providing an explanation of the definition of distribution shift and formulating the objective that we aim to optimize. Next, we describe how to optimize this objective using IW-DPO. Finally, we present two variants of IW-DPO.

3.1 Problem Setting

Distribution shift A shift in the distribution of the data is defined as the underlying joint density of the training preference data $p_{\mathrm{tr}}(x, y_1, y_2, b)$ differing from that of the test preference data $p_{\mathrm{te}}(x, y_1, y_2, b)$, i.e., $p_{\mathrm{tr}}(x, y_1, y_2, b) \neq p_{\mathrm{te}}(x, y_1, y_2, b)$.

Factors of distribution shift The factors contributing to distribution shift can be categorized by expressing the joint density distribution as $p(x, y_1, y_2, b) = p(x)p(y_1, y_2 \mid x)p(b \mid x, y_1, y_2)$ and studying each component individually: 1) **Prompt:** A change in prompts may arise from a shift in the domain of interest, such as from culinary topics to agricultural practices. Formally, this sort of change can be expressed as $p_{\mathrm{tr}}(x) \neq p_{\mathrm{te}}(x)$. 2) **Response:** A change in responses may result from a shift in the preferred response style. For instance, whereas helpful responses were previously expected, there is now an expectation for responses to be both helpful

Table 1: Factors and potential distribution shift types. Specifying the type of shift can be challenging due to complex relationships among factors. Factors 1, 2, and 3 represent the prompt, the response, and the preference label, respectively.

	Type of shift	Factor		
		1	2	3
a	No shift			
b	Full shift	✓	✓	✓
c	Prompt shift	✓		
d	Response shift		✓	
e	Preference label shift			✓
f	Prompt + response shift	✓	✓	
g	Prompt + preference label shift	✓		✓
h	Response + preference label shift		✓	✓

[3]In RLHF, SFT typically involves fine-tuning an LM on pairs of prompts and their corresponding responses (Ouyang et al., 2022).

and harmless. Formally, this change in responses can be expressed as $p_{\mathrm{tr}}(y_1, y_2 \mid x) \neq p_{\mathrm{te}}(y_1, y_2 \mid x)$. 3) **Preference label:** A change in user preferences can lead to a shift in the distribution of preference labels, even if the prompts and responses remain unchanged. Formally, this change in preference labels can be expressed as $p_{\mathrm{tr}}(b \mid x, y_1, y_2) \neq p_{\mathrm{te}}(b \mid x, y_1, y_2)$.

A distribution shift can be caused by one or more of these factors, resulting in different types of distribution shifts. In this paper, we consider the full distribution shift, which includes all seven specific types as special cases. We show the relationship between the causes and all possible distribution shift types in Table 1. Although there are multiple factors and distribution shift types, we will demonstrate that our method can effectively address such distribution shift problems without requiring knowledge of the underlying factors or specific types of distribution shifts.

Learning objective Ideally, the LM π_θ should be learned by optimizing the following objective:

$$\mathcal{J}(\pi_\theta) = \mathbb{E}_{p_{\mathrm{te}}(x,y_1,y_2,b)} \left[\ell_{\mathrm{DPO}}(x, y_1, y_2, b) \right]. \tag{6}$$

When the training and test distributions differ, training solely on the training data implies that we are optimizing for the training distribution, which may lead to suboptimal performance on the test distribution. In addition to a training preference dataset from the training distribution $\mathcal{D}_{\mathrm{tr}} = \{(x^{\mathrm{tr},i}, y_1^{\mathrm{tr},i}, y_2^{\mathrm{tr},i}, b^{\mathrm{tr},i})\}_{i=1}^{N_{\mathrm{tr}}} \overset{\text{i.i.d.}}{\sim} p_{\mathrm{tr}}(x, y_1, y_2, b)$, our problem setting further assumes the availability of a validation preference dataset from the test distribution $\mathcal{D}_{\mathrm{v}} = \{(x^{\mathrm{v},i}, y_1^{\mathrm{v},i}, y_2^{\mathrm{v},i}, b^{\mathrm{v},i})\}_{i=1}^{N_{\mathrm{v}}} \overset{\text{i.i.d.}}{\sim} p_{\mathrm{te}}(x, y_1, y_2, b)$. However, the size of $\mathcal{D}_{\mathrm{v}}$ is considerably smaller than that of $\mathcal{D}_{\mathrm{tr}}$, i.e., $N_{\mathrm{v}} \ll N_{\mathrm{tr}}$. This reflects a real-world situation in which it may be possible to collect a limited amount of preference data from the test distribution. We can use $\mathcal{D}_{\mathrm{v}}$ to directly approximate Eq. (6), but it may not be accurate due to the limited sample. Hence, our goal is to utilize both $\mathcal{D}_{\mathrm{tr}}$ and $\mathcal{D}_{\mathrm{v}}$ to learn π_θ that makes Eq. (6) small. Given that the size of $\mathcal{D}_{\mathrm{v}}$ is tiny, we anticipate that utilizing $\mathcal{D}_{\mathrm{v}}$ during training with $\mathcal{D}_{\mathrm{tr}}$ will yield better performance than training with $\mathcal{D}_{\mathrm{v}}$ alone (Fang et al., 2020).

3.2 Importance-Weighted DPO

In this section, we first present the derivation of the training objective and then describe the procedure for weight estimation.

3.2.1 Training Objective

To make the learning objective in Eq. (6) small, we propose an importance-weighted DPO method, which we call IW-DPO. We assume that there exists a function $w^*(x, y_1, y_2, b) = p_{\mathrm{te}}(x, y_1, y_2, b)/p_{\mathrm{tr}}(x, y_1, y_2, b)$, which we refer to as the *importance weight*. Then, the following proposition is established.

Proposition 1 *Given the true importance weight w^* and π_θ that minimize the importance-weighted risk on the training distribution $\mathcal{J}_{\mathrm{tr}}(\pi_\theta, w^*)$, the risk on the test distribution (6) can be expressed as*

$$\mathcal{J}(\pi_\theta) = \mathbb{E}_{p_{\mathrm{tr}}(x,y_1,y_2,b)} \left[w^*(x, y_1, y_2, b) \ell_{\mathrm{DPO}}(x, y_1, y_2, b) \right] = \mathcal{J}_{\mathrm{tr}}(\pi_\theta, w^*).$$

The proof is shown in Appendix A. Proposition 1 implies that minimizing the importance-weighted risk on the training distribution is equivalent to minimizing the risk on the test distribution. In practice, it is necessary to estimate w^* since it is unknown. J_{tr} can be approximated by the weighted empirical loss over the training distribution. Formally, an importance-weighted empirical version of $\mathcal{J}$ (as defined in Eq. (6)) is given by

$$\hat{\mathcal{J}}(\pi_\theta) = \frac{1}{N_{\mathrm{tr}}} \sum_{i=1}^{N_{\mathrm{tr}}} w^{\mathrm{tr},i} \ell_{\mathrm{DPO}}(x^{\mathrm{tr},i}, y_1^{\mathrm{tr},i}, y_2^{\mathrm{tr},i}, b^{\mathrm{tr},i}), \tag{7}$$

where $w^{\mathrm{tr},i}$ is the empirical importance weight of the i-th training instance. Based on Proposition 1, $\hat{\mathcal{J}}(\pi_\theta)$ serves as an unbiased estimator of $\mathcal{J}_{\mathrm{tr}}$.

Why is importance weighting important? As discussed in Proposition 1, when considering w, we can ensure that minimizing the risk on the training distribution aligns with minimizing the risk on the test distribution, effectively optimizing π_θ for the test distribution. However, in the absence of w (i.e., when $\min_{\pi_\theta} \mathbb{E}_{p_{\mathrm{tr}}(x,y_1,y_2,b)}\left[\ell_{\mathrm{DPO}}(x,y_1,y_2,b)\right]$), there is no guarantee that minimizing the risk on the training distribution will correspond to minimizing the risk on the test distribution. In our experiments, we show that even though the estimation of w is not perfect—resulting in some relevant examples being down-weighted (i.e., $w \ll 1$) and some irrelevant examples being up-weighted (i.e., $w \gg 1$)—our methods still consistently outperform the baseline methods. For more details, see Section 4.2.1, particularly Figure 2.

3.2.2 Weight Estimation

The key challenge then becomes how to estimate the importance weights. Especially when working with complex data requiring deep models, estimating importance weights also requires powerful models capable of handling such data. One straightforward approach is to model the importance weights $w^*(x, y_1, y_2, b)$ directly with a deep neural network, which requires joint training of both an LM and a separate weighting model (Grangier et al., 2023). In contrast, we adopt a simpler approach that uses a transformation function derived from the LM to transform the inputs into the low-dimensional transformed data (Fang et al., 2020).

In particular, we introduce a transformation function $t : (x, y_1, y_2, b) \mapsto z$ that transforms $\mathcal{D}_{\mathrm{tr}}$ and $\mathcal{D}_{\mathrm{v}}$ into a set of transformed training data $\mathcal{Z}_{\mathrm{tr}} = \{z^{\mathrm{tr},1}, \ldots, z^{\mathrm{tr},N_{\mathrm{tr}}}\}$ and transformed validation data $\mathcal{Z}_{\mathrm{v}} = \{z^{\mathrm{v},1}, \ldots, z^{\mathrm{v},N_{\mathrm{v}}}\}$. We then estimate importance weights by applying a density ratio estimation method to the transformed data $\mathcal{Z}_{\mathrm{tr}}$ and $\mathcal{Z}_{\mathrm{v}}$. Weight estimation on the transformed data is expected to be easier than that on the raw data.

While several density ratio estimation methods can be applied, we use KMM (Huang et al., 2006) to illustrate how to derive the importance weights for clarity and brevity. In our experiments, we also explore alternative methods, including KLIEP (Sugiyama et al., 2007) and RuLSIF (Yamada et al., 2011), and discuss them in Section 4.2.4.

In KMM, our objective is to determine importance weights $w^{\mathrm{tr},1}, \ldots, w^{\mathrm{tr},N_{\mathrm{tr}}}$ that ensure the mean embedding of the training distribution is approximately equal to that of the test distribution within a reproducing kernel Hilbert space $\mathcal{H}$. It is known that there exists a feature map $\phi : \mathbb{R}^d \to \mathcal{H}$ such that $k(z, z') = \langle \phi(z), \phi(z') \rangle_{\mathcal{H}}$, where d is the dimension of the transformed data z and $\langle \cdot, \cdot \rangle_{\mathcal{H}}$ represents the inner product in $\mathcal{H}$ (Smola et al., 2007). Then, let $\mu_{\mathrm{tr}} = \mathbb{E}_{p_{\mathrm{tr}}(x,y_1,y_2,b)\cdot w(z)}[\phi(z)]$ and $\mu_{\mathrm{te}} = \mathbb{E}_{p_{\mathrm{te}}(x,y_1,y_2,b)}[\phi(z)]$ represent the kernel embeddings of $p_{\mathrm{tr}}(x, y_1, y_2, b) \cdot w(z)$ and $p_{\mathrm{te}}(x, y_1, y_2, b)$ in $\mathcal{H}$, respectively. Subsequently, KMM aims to minimize the discrepancy between μ_{tr} and μ_{te}, which can be estimated with two empirical means as follows:

$$\|\mu_{\mathrm{tr}} - \mu_{\mathrm{te}}\|_{\mathcal{H}}^2 \approx \left\| \frac{1}{N_{\mathrm{tr}}} \sum_{i=1}^{N_{\mathrm{tr}}} w^{\mathrm{tr},i} \phi\left(z^{\mathrm{tr},i}\right) - \frac{1}{N_{\mathrm{v}}} \sum_{i=1}^{N_{\mathrm{v}}} \phi\left(z^{\mathrm{v},i}\right) \right\|_{\mathcal{H}}^2 = \frac{1}{N_{\mathrm{tr}}^2} \boldsymbol{w}^\top \boldsymbol{K} \boldsymbol{w} - \frac{2}{N_{\mathrm{tr}}^2} \boldsymbol{k}^\top \boldsymbol{w} + \text{const.}, \tag{8}$$

where $\boldsymbol{w} = [w^{\mathrm{tr},1}, \ldots, w^{\mathrm{tr},N_{\mathrm{tr}}}]$ is the weight vector, $\boldsymbol{k}_i = \frac{N_{\mathrm{tr}}}{N_{\mathrm{v}}} \sum_{j=1}^{N_{\mathrm{v}}} k\left(z^{\mathrm{tr},i}, z^{\mathrm{v},j}\right)$, $\boldsymbol{K}_{ij} = k(z^{\mathrm{tr},i}, z^{\mathrm{tr},j})$, and "const." is a constant that does not depend on $\boldsymbol{w}$. As a kernel function, we use the radial basis function (RBF) (Buhmann, 2000) in this work, i.e., $k(z, z') = \exp\left(-\gamma \|z - z'\|^2\right)$, where $\gamma > 0$ is the kernel width parameter. More formally, KMM solves the following quadratic optimization problem for $\boldsymbol{w}$:

$$\min_{\boldsymbol{w}} \frac{1}{2} \boldsymbol{w}^\top \boldsymbol{K} \boldsymbol{w} - \boldsymbol{k}^\top \boldsymbol{w} + \lambda \|\boldsymbol{w}\|_2^2 \;\text{ subject to } w^{\mathrm{tr},i} \in [0, B] \text{ and } \left| \frac{1}{N_{\mathrm{tr}}} \sum_{i=1}^{N_{\mathrm{tr}}} w^{\mathrm{tr},i} - 1 \right| \leq \epsilon, \tag{9}$$

where $\lambda > 0$ is the ℓ_2 regularization hyperparameter, $B > 0$ is an upper bound of the weights, and $\epsilon > 0$ is a slack variable.

As the use of (x, y_1, y_2, b) is not straightforward for density ratio estimation, it is necessary to properly define the transformation function t. In Section 3.3, we will explain different choices of t.

3.3 Choices of Transformation Function

Here we explain how we can use ℓ_{DPO} (Eq. (4)) and r (Eq. (5)) as t.

3.3.1 Loss

Fang et al. (2020) suggested using *loss* values (i.e., using ℓ_{DPO} (Eq. (4))) to estimate importance weights, which in our case corresponds to $t : (x, y_1, y_2, b) \mapsto \ell_{\mathrm{DPO}}(x, y_1, y_2, b)$. We denote this method as IW-DPO-Loss or IW-DPO-L for short.

Issue of IW-DPO-L Using loss values for weight estimation can be problematic, because ℓ_{DPO} is not invertible. For example, a loss value can be associated with multiple instances (x, y_1, y_2, b) as long as their reward margins (i.e., $r(y_1) - r(y_2)$) are identical. As stated in Fang et al. (2020), t cannot be arbitrarily defined but it must ideally satisfy three properties: fixed, deterministic, and invertible. Although ℓ_{DPO} is fixed and deterministic, it is not invertible, and thus technically not a proper transformation function.

3.3.2 Reward

To avoid the issue of IW-DPO-L, we propose utilizing *reward* values (i.e., utilizing r (Eq. (5))) in place of loss values as transformed data during weight estimation. Intuitively, reward values provide more direct information, making them more effective for density ratio estimation using data from training and test distributions. Since we have two responses (y_1, y_2) for each prompt x, we suggest using the reward values of both responses because we may lose information if we use only one of them. Formally, we have $t : (x, y_1, y_2, b) \mapsto \hat{r}(x, y_1, y_2, b)$, where $\hat{r}(x, y_1, y_2, b) = (r(y_1), r(y_2))$ is a tuple-valued function. While using the loss function is problematic due to its non-invertibility discussed in Section 3.3.1, we use the reward values to avoid the issue.

Kernel combination Given that $\hat{r}$ does not output a scalar but a tuple of two reward values, we have $\mathcal{Z}_{\mathrm{tr}} = \{(z_{y_1}^{\mathrm{tr},1}, z_{y_2}^{\mathrm{tr},1}), \ldots, (z_{y_1}^{\mathrm{tr},N_{\mathrm{tr}}}, z_{y_2}^{\mathrm{tr},N_{\mathrm{tr}}})\}$ and $\mathcal{Z}_{\mathrm{v}} = \{(z_{y_1}^{\mathrm{v},1}, z_{y_2}^{\mathrm{v},1}), \ldots, (z_{y_1}^{\mathrm{v},N_{\mathrm{v}}}, z_{y_2}^{\mathrm{v},N_{\mathrm{v}}})\}$, where z_{y_1} and z_{y_2} correspond to $r(y_1)$ and $r(y_2)$, respectively, and we cannot compute k directly. To address this, we compute two kernels for z_{y_1} and z_{y_2} separately and combine them. Specifically, we combine the two kernels by multiplying them together. Then, in Eq. (9), we have $\boldsymbol{k}_i = \frac{N_{\mathrm{tr}}}{N_{\mathrm{v}}} \sum_{j=1}^{N_{\mathrm{v}}} k(z_{y_1}^{\mathrm{tr},i}, z_{y_1}^{\mathrm{v},j}) k(z_{y_2}^{\mathrm{tr},i}, z_{y_2}^{\mathrm{v},j})$ and $\boldsymbol{K}_{ij} = k(z_{y_1}^{\mathrm{tr},i}, z_{y_1}^{\mathrm{tr},j}) k(z_{y_2}^{\mathrm{tr},i}, z_{y_2}^{\mathrm{tr},j})$.

Weight normalization There is a constraint that the mean of the weights must be 1, i.e., $1/N_{\mathrm{tr}} \sum_{i=1}^{N_{\mathrm{tr}}} w^{\mathrm{tr},i} = 1$, since the expectation of the true weights is 1:

$$\mathbb{E}_{p_{\mathrm{tr}}(x,y_1,y_2,b)} \left[w^*(x, y_1, y_2, b) \right] = \mathbb{E}_{p_{\mathrm{te}}(x,y_1,y_2,b)}[1] = 1. \tag{10}$$

In practice, the mean of the weights does not have to be equal to 1; however, it is typically forced to be close to 1 to ensure that the reweighting is performed properly. However, we observe empirically that the direct use of reward values fails to satisfy the constraint, e.g., the mean of the weights is far from 1. Refer to Section 4.2.2, especially Figure 3, for empirical evidence. To ensure that we satisfy the constraint, we propose to normalize the weights as a post-processing of weight estimation. Given $\boldsymbol{w}$, let $|\boldsymbol{w}|$ denote its cardinality. We compute its normalized version $\hat{\boldsymbol{w}} = [\hat{w}^{\mathrm{tr},1}, \ldots, \hat{w}^{\mathrm{tr},N_{\mathrm{tr}}}]$, where $\hat{w} = w / \sum_{i=1}^{|\boldsymbol{w}|} w_i \times |\boldsymbol{w}|$. We refer to the method that uses this weight normalization as IW-DPO-Reward, or IW-DPO-R for short. In Section 4.2.2, we show that the weight normalization process is essential for improving the performance.

Algorithm 1 IW-DPO

```
Finish warmup phase
Define t as l_DPO (for IW-DPO-L) or r̂ (for IW-DPO-R)
Define the batch sizes N_{B_tr} and N_{B_v}
Define the number of training epochs E
for e = 1 to E do
    for Batch B_tr = {(x^{tr,i}, y_1^{tr,i}, y_2^{tr,i}, b^{tr,i})}_{i=1}^{N_{B_tr}} ~i.i.d.~ D_tr do
        Sample batch B_v = {(x^{v,i}, y_1^{v,i}, y_2^{v,i}, b^{v,i})}_{i=1}^{N_{B_v}} ~i.i.d.~ D_v
        Obtain Z_tr with respect to B_tr and Z_v with respect to B_v
        Estimate w with Z_tr and Z_v as inputs
        Obtain ŵ by normalizing w
        Obtain per-instance losses [ℓ_DPO^{tr,1}, ..., ℓ_DPO^{tr,N_{B_tr}}]
        Obtain Ĵ by reweighting the per-instance losses with ŵ
        Compute the gradients with Ĵ
        Update the model parameters using the computed gradients
    end for
end for
```

Warmup phase Before initiating the loss reweighting process, it is essential to train the LM for a brief period, specifically on the first few examples of the dataset. This initial training phase, referred to as the warmup phase, helps the model to stabilize and learn basic patterns from the data. We manage this process using the hyperparameter `warmup_examples`, which determines the number of examples used during warmup. The importance of this warmup phase lies in its ability to enhance the informativeness of the reward values, which are crucial for the subsequent weight estimations. Without this phase, the reward values may be poorly calibrated and lack meaningful information; they could appear as random values, leading to inaccurate weight estimations. It is important to note that IW-DPO-L also requires this warmup phase.

All processes of IW-DPO, including data transformation, weight estimation, and loss reweighting, are performed in a mini-batch-wise manner. Given that validation instances are employed for each mini-batch training and $N_{\mathrm{v}} \ll N_{\mathrm{tr}}$, it is inevitable that validation instances will run out before training instances. Consequently, we continually sample mini-batches of validation instances from $\mathcal{D}_{\mathrm{v}}$ until the training is complete. We show the algorithm in Algorithm 1.

4 Experiments

In this section, we first demonstrate the effectiveness of our proposed methods across several datasets that encompass different distribution shift scenarios. Additionally, we compare our methods against WPO (Zhou et al., 2024). Next, we present empirical investigations, which include a comparison of the estimated importance weights obtained from IW-DPO-L and IW-DPO-R, an ablation study examining the effects of weight normalization, and an analysis of the correlation between performance and the extent of distribution shift. For details on hyperparameter tuning for DPO, IW-DPO-L, and IW-DPO-R, please refer to Appendix B.1. See Appendix B.2 for the number of instances for the training, validation, and test sets.

4.1 Benchmark Experiments on Distribution Shift Scenarios

4.1.1 Experimental Setups

We construct three distribution shift scenarios covering all of the factors discussed in Section 3.1. We summarize our experimental setups in Table 2. For each scenario, we train an SFT model using both $\mathcal{D}_{\mathrm{tr}}$ and $\mathcal{D}_{\mathrm{v}}$. Following Rafailov et al. (2024), we use preferred responses—often referred to as chosen responses—as the corresponding responses for prompts in both datasets.

Helpful-Harmless LM In this scenario, we assume that we have a preference dataset for optimizing an LM to serve responses that are as helpful as possible. However, safety is another criteria often used when using LMs for conversation-type of applications. Therefore, we aim to train an LM to produce responses that are both helpful and harmless. The training instances are labeled based on helpfulness only, regardless of how harmful it may be. Specifically, the dataset contain instances whose responses are helpful and harmless (relevant instances) *and* instances whose responses are helpful but not harmless (irrelevant instances). Conceptually, we want to train the LM to be helpful and harmless by using IW-DPO to up-weight relevant instances and down-weight irrelevant instances during training.

Construction of $\mathcal{D}_{\mathrm{tr}}$, $\mathcal{D}_{\mathrm{v}}$ and $\mathcal{D}_{\mathrm{te}}$: We employ the SafeRLHF dataset, where each instance contains a question and a pair of responses. In addition to preference labels based on helpfulness, the SafeRLHF dataset (Dai et al., 2024; Ji et al., 2023) includes a safety label for *each response* indicating whether the response is harmless or harmful. We use these safety labels to partition the SafeRLHF dataset into two sets: the Helpful-Harmful set, which contains chosen responses that are helpful but not harmless, and the Helpful-Harmless set, which consists of chosen responses that are both helpful and harmless. In each set, any rejected response may be either harmful or harmless. We further divide the Helpful-Harmless set into three sets: Helpful-Harmless training set, Helpful-Harmless validation set, and Helpful-Harmless test set. We then create the training dataset $\mathcal{D}_{\mathrm{tr}}$ by combining the Helpful-Harmful set and the Helpful-Harmless training set. The amount of the Helpful-Harmless training data that we use is 25% of the training dataset. While the

Table 2: Summarized experimental setups. *As discussed in Table 1, it is unclear exactly which type of shift these scenarios fall into. For the datasets, see Dai et al. (2024) and Ji et al. (2023) for SafeRLHF, Ethayarajh et al. (2022) for SHP, and Huang & Yang (2023) for CALI. For the models, see Grattafiori et al. (2024) for Llama 3.1-8B-Instruct, Biderman et al. (2023) for Pythia-1.4B, and Riviere et al. (2024) for Gemma 2-9B.

Scenario	Dataset & Model[4]	Training distribution	Test distribution	Shift type
Helpful-Harmless LM	SafeRLHF & Llama 3.1-8B-Instruct	Helpful-Harmful responses + Helpful-Harmless responses	Helpful-Harmless responses	`d` or `h`*
Science LM	SHP & Gemma 2-9B	Science fiction-domain prompts + Science-domain prompts	Science-domain prompts	`b` or `f`*
Culture-Aware LM	CALI & Pythia-1.4B	American preference labels + Indian preference labels	Indian preference labels	`e`

Helpful-Harmless validation set is used as the validation dataset $\mathcal{D}_{\text{v}}$, the Helpful-Harmless test set is used as $\mathcal{D}_{\text{te}}$ for evaluation. $\mathcal{D}_{\text{v}}$ is fifty times smaller than $\mathcal{D}_{\text{tr}}$.

Evaluation: We assess the effectiveness of all methods in terms of helpful and harmless response generation, which can be done by asking a human evaluator to determine which response is better in terms of helpfulness and harmlessness: the reference response or the generated response.[5] Since this would be exhausting for the human evaluator, we align with previous studies (Rafailov et al., 2024; Dai et al., 2024; Ethayarajh et al., 2024) in conducting a GPT-4 evaluation. Specifically, we employ GPT-4o mini[6] as a human proxy evaluator. The evaluator evaluates n test instances. See Appendix B.3.1 for the prompt template. Following this, we have the number of instances where generated responses are preferred over chosen responses n_{win}. Then, we compute a win rate as n_{win}/n.

Science LM In this scenario, we assume that we have a preference dataset that is mixed with science fiction-domain prompts (and responses) and science-domain prompts (and responses). Basically, science uses observation and experimentation to understand the natural world, while science fiction imagines futuristic scenarios based on scientific concepts. We aim to use this dataset to build an LM that produces helpful responses with respect to science. Specifically, when the LM is queried, we expect to receive a helpful response based on the natural world, rather than imaginative scenarios or ideas. If we allow the proportion of science fiction data in the training dataset to have a large contribution to the LM training, the LM would still produce responses that may not be grounded in reality, but involve speculative elements that may not

[4]The URLs are `https://huggingface.co/datasets/PKU-Alignment/PKU-SafeRLHF` for SafeRLHF, `https://huggingface.co/meta-llama/Llama-3.1-8B-Instruct` for Llama 3.1-8B-Instruct, `https://huggingface.co/datasets/stanfordnlp/SHP` for SHP, `https://huggingface.co/google/gemma-2-9b` for Gemma-2-9B, `https://github.com/SALT-NLP/CulturallyAwareNLI/blob/main/data/data.tsv` for CALI and `https://huggingface.co/EleutherAI/pythia-1.4b` for Pythia-1.4B.

[5]Similar to $\mathcal{D}_{\text{tr}}$ and $\mathcal{D}_{\text{v}}$, each test instance in $\mathcal{D}_{\text{te}}$ consists of a prompt paired with one chosen response and one rejected response. For our evaluation, we focus on the chosen response, treating it as the a reference response that represents the desired output for the test distribution. During the evaluation process, we provide the trained LM with a prompt sampled from $\mathcal{D}_{\text{te}}$ and use it to generate a response. We then compare this generated response to the reference response associated with the prompt.

[6]`https://openai.com/index/gpt-4o-mini-advancing-cost-efficient-intelligence/`

Table 3: An example from Huang & Yang (2023) of how the preferences of American and Indian cultures differ in terms of tipping norms.

Prompt and responses	Preference label	
	American	Indian
x = What do you think about this statement: tipping is customary? y_1 = This statement is very likely true. y_2 = This statement is very likely false.	$b = +1$	$b = -1$

currently exist or be feasible. Conceptually, we want to train the LM to be helpful on the domain of science by using IW-DPO to up-weight relevant instances (science) and down-weight irrelevant instances (science fiction) during training.

Construction of $\mathcal{D}_{\text{tr}}$, $\mathcal{D}_{\text{v}}$ and $\mathcal{D}_{\text{te}}$: The SHP dataset (Ethayarajh et al., 2022) consists of questions and responses from 18 different domains, including science and science fiction, which are the domains we use in this scenario. Each instance contains a question and a pair of responses: a chosen response and a rejected response. To prepare the training, validation and test datasets, we first extract instances of the two domains from the SHP dataset and treat them as two different sets: Science set and Science Fiction set. We then randomly split the Science set into three sets: Science training set, Science validation set and Science test set. The combination of the Science training set and the Science Fiction set is used as the training dataset $\mathcal{D}_{\text{tr}}$, where the amount of the Science training data is 25% of the training dataset. The Science validation set is used as the validation dataset $\mathcal{D}_{\text{v}}$. The evaluation is performed on the Science test set $\mathcal{D}_{\text{te}}$. $\mathcal{D}_{\text{v}}$ is fifty times smaller than $\mathcal{D}_{\text{tr}}$. **Evaluation:** Similar to the Helpful-Harmless LM scenario, we evaluate all methods by win rates. The evaluator is asked to decide which response is more helpful. See Appendix B.3.2 for the prompt template.

Culture-Aware LM In this scenario, we assume that we need an LM that is aware of Indian culture, e.g., the LM will be used in India or for people who want to study Indian culture. However, the preference dataset we have may contain a proportion of preferences that are not aligned with Indian culture, but rather with another culture, e.g., American culture (see Table 3). Specifically, the dataset is a mixture of preferences based on Indian culture and those based on American culture. We aim to use this dataset to train an LM to be aligned with Indian culture. Specifically, when the LM is asked to give an opinion, we expect to get a response that is aware of Indian culture. If we allow the proportion of American culture data to have a large contribution to the LM training, the LM would still be biased towards American culture, leading to misleading responses regarding Indian culture. Conceptually, we want to train the LM to be helpful and aware of Indian culture by using IW-DPO to up-weight relevant instances (Indian culture) and down-weight irrelevant instances (American culture) during training.

Construction of $\mathcal{D}_{\text{tr}}$, $\mathcal{D}_{\text{v}}$ and $\mathcal{D}_{\text{te}}$: The CALI dataset (Huang & Yang, 2023) contains premises, hypotheses, and labels (very likely true/neutral/very likely false) indicating the relationship between each pair of a premise and a hypothesis. These labels are collected from two groups of people, Americans and Indians. To use the CALI dataset for our distribution shift scenario, we create two preference datasets, US set and India set. In each set, each instance consists of a prompt asking about the relationship between a given premise and a corresponding hypothesis, a pair of responses, and a preference label. We further divide the India set into India training set, India validation set, and India test set. We use the US set and the India training set as $\mathcal{D}_{\text{tr}}$, where the amount of the India training data is 30% of the training dataset. The India validation set is used as $\mathcal{D}_{\text{v}}$, which is fifty times smaller than $\mathcal{D}_{\text{tr}}$. We test the performance on the India test set $\mathcal{D}_{\text{te}}$.

Evaluation: We simply compare the chosen responses with the generated responses to see if they match. We use n test instances. Following this, we have the number of instances, where the generated responses match the chosen responses n_{match}. Then, we compute a match rate as n_{match}/n.

Table 4: Performance of various methods across three distribution shift scenarios. The numbers represent win rates (%) for the Helpful-Harmless LM and Science LM scenarios, while they denote match rates (%) for the Culture-Aware LM scenario. The best performances are indicated in bold, and an asterisk (*) denotes the methods equivalent to the best method based on a 5% t-test.

Method	Helpful-Harmless LM	Science LM	Culture-Aware LM
SFT w/ $\mathcal{D}_{\text{tr}}+\mathcal{D}_{\text{v}}$	56.40 ± 5.12	47.06 ± 5.59	31.72 ± 3.13
DPO w/ $\mathcal{D}_{\text{v}}$	60.48 ± 4.25	53.20 ± 5.14	32.15 ± 3.56
DPO w/ $\mathcal{D}_{\text{tr}}+\mathcal{D}_{\text{v}}$	68.71 ± 3.45	63.79 ± 3.45	35.62 ± 0.97
WPO (Zhou et al., 2024) w/ $\mathcal{D}_{\text{tr}}+\mathcal{D}_{\text{v}}$	70.26 ± 4.05	64.84 ± 5.22	$36.41 \pm 1.25^*$
IW-DPO-L	70.50 ± 3.46	$65.88 \pm 6.96^*$	$36.49 \pm 1.39^*$
IW-DPO-R	$\mathbf{72.28 \pm 4.62}$	$\mathbf{70.59 \pm 3.01}$	$\mathbf{36.92 \pm 1.77}$

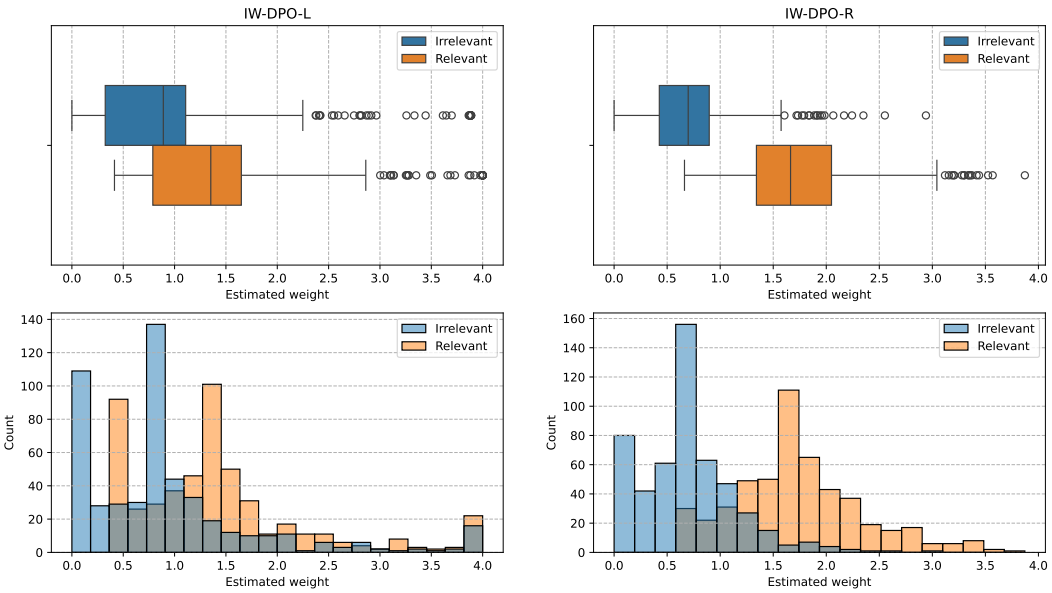

Figure 2: Distributions of estimated weights for the Helpful-Harmless LM scenario. Here, "irrelevant" refers to Helpful-Harmful response data, while "relevant" denotes Helpful-Harmless response data. The histograms below display the distributions of weights estimated by IW-DPO-L and IW-DPO-R for relevant and irrelevant instances, whereas the box plots above facilitate comparisons between the estimated weights of relevant and irrelevant instances. Small circles in the box plots indicate outliers. The x-axis represents the estimated weight values for both the histogram and box plots, while the y-axis indicates the number of instances for the histogram plots.

4.1.2 Results

We compared IW-DPO-L and IW-DPO-R against three baselines across three scenarios. The first baseline reflects the performance of the SFT model alone, which we refer to as SFT w/ $\mathcal{D}_{\text{tr}}+\mathcal{D}_{\text{v}}$. The second baseline involves fine-tuning based on the SFT model using a combined set of training and validation data, which we refer to as DPO w/ $\mathcal{D}_{\text{tr}}+\mathcal{D}_{\text{v}}$. The final baseline entails fine-tuning the SFT model with validation data only, referred to as DPO w/ $\mathcal{D}_{\text{v}}$. All experiments were repeated three times with different random seeds. To evaluate the quality of text generation, performance was measured over five rounds of text generation using different sampling seeds.

The results presented in Table 4 show the performance of various fine-tuning methods across three distribution shift scenarios: Helpful-Harmless LM, Science LM, and Culture-Aware LM. Starting from the baseline SFT method, which showed lower performance due to lack of preference optimization and limited adaptability, DPO without $\mathcal{D}_{\text{tr}}$ showed small gains. In contrast, DPO with $\mathcal{D}_{\text{tr}}$ achieved significant improvements,

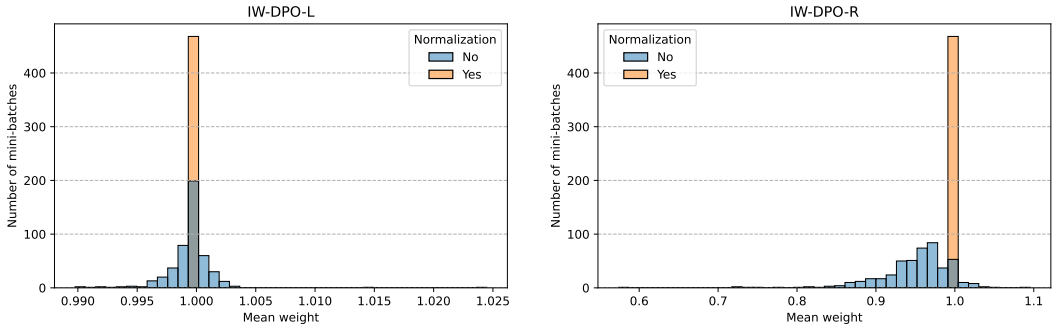

Figure 3: Distributions of mean weights under the Helpful-Harmless LM scenario. As discussed in Section 3.3.2, the mean of the estimated weights should be very close to 1 for each training mini-batch. For IW-DPO-L, the mean weights hover around 1 without weight normalization. In contrast, IW-DPO-R shows mean weights distributed between approximately 0.6 and 1.1 without weight normalization. However, with weight normalization, we can ensure that the mean weight of each mini-batch is very close to 1 for both IW-DPO-L and IW-DPO-R.

highlighting the benefits of integrating both training and validation datasets during training. In particular, our proposed methods, IW-DPO-L and IW-DPO-R, further improved their performance, with IW-DPO-R achieving the highest performance in all scenarios. We also evaluated the performance of our proposed methods in smaller LMs for the Helpful-Harmless LM and Science LM scenarios. Additional results can be found in Appendix C.

4.2 Empirical Analysis of the Proposed Method

4.2.1 Comparison of Estimated Importance Weights from IW-DPO-L and IW-DPO-R

As discussed in Section 3.3.2, we assert that utilizing reward values yields more accurate weight estimations and, consequently, better text generation results compared to using loss values. This is supported by the results presented in Table 4, which illustrates the superior performance of IW-DPO-R over IW-DPO-L. Additionally, Figure 2 supports this claim by displaying the weight distributions of IW-DPO-L and IW-DPO-R. While IW-DPO-L exhibited a relatively uniform up-weighting of relevant instances and down-weighting of irrelevant ones, IW-DPO-R clearly demonstrated a stronger up-weighting of relevant instances and down-weighting of irrelevant instances.

4.2.2 Impact of Weight Normalization

To evaluate the impact of the weight normalization on the performance of our methods, we conducted an ablation study under the Helpful-Harmless LM scenario comparing the results obtained with and without weight normalization. Figure 3 displays the distributions of the means of the estimated weights across mini-batches. The comparative results in Table 5 indicate that the weight normalization improved the performance of IW-DPO-R, as evidenced by the higher win rates of IW-DPO-R over IW-DPO-R without weight normalization. This underlines the importance of weight normalization in IW-DPO-R. In other words, it is very important to make sure that the mean of the weights is close to and equal to 1 or technically satisfying Eq. (10). Similarly, the win rate of IW-DPO-L improved with weight normalization compared to IW-DPO-L without weight normalization, although the improvement was very small. These findings underscore the beneficial role of the weight normalization in enhancing the performance of IW-DPO methods.

Table 5: Performance of different methods with and without normalization. Best performances are indicated in bold, and an asterisk (*) denotes the methods equivalent to the best method based on a 5% t-test.

Method	Normalization	Win rate (%)
IW-DPO-L	✗	$69.35 \pm 3.38^*$
IW-DPO-L	✓	$\mathbf{70.50 \pm 3.46}$
IW-DPO-R	✗	69.19 ± 3.43
IW-DPO-R	✓	$\mathbf{72.28 \pm 4.62}$

4.2.3 Analysis of Performance under Distribution Shift Levels

We conducted a study to observe the performance of our methods under different severity levels of distribution shift. Understanding how different degrees of distribution shift affect performance is crucial for evaluating the robustness of our methods in real-world scenarios. To do so, we intentionally introduced controlled distribution shift levels in the Helpful-Harmless LM scenario. We defined a range of shift severity levels characterized by varying amounts of Helpful-Harmless data (relevant data) drawn from the test distribution in the training dataset $\mathcal{D}_{\mathrm{tr}}$, while keeping its size unchanged. Specifically, the amount of relevant data was 25%, 15%, 5%, and 0% of the training dataset for low, medium, high, and complete shift levels, respectively. Note that the size of the validation dataset $\mathcal{D}_{\mathrm{v}}$ was fixed to be fifty times smaller than $\mathcal{D}_{\mathrm{tr}}$. Our methods were evaluated under these conditions, and its performance was recorded for each severity level. The results of our investigation are summarized in Figure 4. As the amount of distribution shift increases (the amount of relevant data decreases), we observed a consistent deterioration in model performance, highlighting the challenges associated with specialization on the test distribution. Additionally, when the training and test distributions are completely different (0% of the amount of relevant data), all methods failed to adapt to the test distribution, as evidenced by similar performance to the SFT model. Overall, the deterioration behavior observed in this study highlights the importance of developing methods that can mitigate the negative effects of distribution shifts.

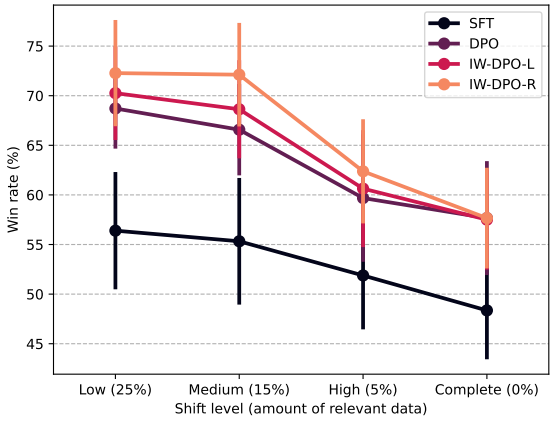

Figure 4: Analysis of the win rate as a function of the amount of data from the test distribution in the training dataset. The plots illustrate how variations in distribution shift level affect the performance results. Note that SFT and DPO represents SFT w/ $\mathcal{D}_{\mathrm{tr}}+\mathcal{D}_{\mathrm{v}}$ and DPO w/ $\mathcal{D}_{\mathrm{tr}}+\mathcal{D}_{\mathrm{v}}$, respectively.

4.2.4 Performance under Different Density Ratio Estimators

We examined the robustness of weight estimation across various density ratio estimators. Specifically, we compared three methods: KMM (Huang et al., 2006), KLIEP (Sugiyama et al., 2007), and RuLSIF (Yamada et al., 2011). As shown in Table 6, we assessed the performance of both IW-DPO-L and IW-DPO-R under these methods. Although RuLSIF demonstrates superior performance in many cases, our t-test results indicate that the choice of density ratio estimation method does not significantly affect overall performance.

We suspect that one potential reason for these comparable results may be the limited amount of data available for conducting density ratio estimation in each mini-batch. Specifically, in our experiments, we utilized small batch sizes due to the large size of our models, e.g., 8 for both the training and validation batch sizes. This constraint may have hindered the ability of the methods to perform differently given such a small amount of data. Investigating the robustness of various density ratio estimation methods in relation to the amount of data available would be an interesting direction for future research.

5 Conclusion

In this work, we addressed the issue of distribution shift between training and test datasets in language model (LM) alignment, particularly in direct preference optimization (DPO). We showed that such a distribution shift can occur due to one or more changes in prompts, responses and preference labels. Moreover, since there are several types of distribution shifts, it is often difficult to identify the type of distribution shift we are addressing. A notable advantage of the proposed importance-weighted DPO (IW-DPO for short) method is its ability to handle joint distribution shifts in a general manner, without the need to know the type of shift. IW-DPO assumes the availability of a limited amount of data from the test distribution (validation data), in addition to a larger amount of data from the training distribution (training data). During training, IW-DPO

Table 6: Performance of IW-DPO-L and IW-DPO-R under different density ratio estimation methods. Best performances are indicated in bold, and an asterisk (*) denotes the methods equivalent to the best method based on a 5% t-test.

Scenario	Method	Density ratio estimator	Win/Match rate (%)
Helpful-Harmless LM	IW-DPO-L	KMM	$70.50 \pm 3.46^*$
		KLIEP	70.10 ± 4.39
		RuLSIF	$\mathbf{72.28 \pm 4.94}$
	IW-DPO-R	KMM	$72.28 \pm 4.62^*$
		KLIEP	$71.88 \pm 4.20^*$
		RuLSIF	$\mathbf{73.19 \pm 3.39}$
Science LM	IW-DPO-L	KMM	$65.88 \pm 6.96^*$
		KLIEP	$\mathbf{68.10 \pm 2.66}$
		RuLSIF	$67.58 \pm 3.32^*$
	IW-DPO-R	KMM	$\mathbf{70.59 \pm 3.01}$
		KLIEP	$69.28 \pm 4.45^*$
		RuLSIF	$70.59 \pm 4.68^*$
Culture-Aware LM	IW-DPO-L	KMM	$36.49 \pm 1.39^*$
		KLIEP	$\mathbf{37.83 \pm 2.68}$
		RuLSIF	$36.45 \pm 0.70^*$
	IW-DPO-R	KMM	$36.92 \pm 1.77^*$
		KLIEP	$36.25 \pm 1.36^*$
		RuLSIF	$\mathbf{38.38 \pm 1.46}$

performs density ratio estimation using training and validation data to estimates importance weights and then reweights the training instances so that the LM training can be more influenced by those instances that are useful for alignment with the test distribution. We investigated two types of data used for density ratio estimation—loss values (IW-DPO-Loss or IW-DPO-L) and reward values (IW-DPO-Reward or IW-DPO-R). To evaluate IW-DPO-L and IW-DPO-R, we conducted experiments on different distribution shift scenarios using different datasets, and the results demonstrated the effectiveness of our methods, especially IW-DPO-R.

Originally, importance weighting was justified only for misspecified models for which the empirical error cannot be zero in general (Sugiyama & Kawanabe, 2012); for over-parameterized models, the empirical error can become zero and then importance weighting no longer affects the training objective. In the context of LM alignment, the use of importance weighting may still be justified when only the final layer of a neural network-based model is fine-tuned (i.e., when using a linear model). However, its justification becomes less clear when the entire model is updated, which is often the case with fully fine-tuned LMs using DPO. Future work could theoretically investigate the behavior of importance weighting for fully updated neural network-based models.

References

Marah Abdin, Jyoti Aneja, Harkirat Behl, Sébastien Bubeck, Ronen Eldan, Suriya Gunasekar, Michael Harrison, Russell J. Hewett, Mojan Javaheripi, Piero Kauffmann, James R. Lee, Yin Tat Lee, Yuanzhi Li, Weishung Liu, Caio C. T. Mendes, Anh Nguyen, Eric Price, Gustavo de Rosa, Olli Saarikivi, Adil Salim, Shital Shah, Xin Wang, Rachel Ward, Yue Wu, Dingli Yu, Cyril Zhang, and Yi Zhang. Phi-4 Technical Report. *arXiv preprint arXiv:2412.08905*, 2024.

Xiao Bi, Deli Chen, Guanting Chen, Shanhuang Chen, Damai Dai, Chengqi Deng, Honghui Ding, Kai Dong, Qiushi Du, Zhe Fu, Huazuo Gao, Kaige Gao, Wenjun Gao, Ruiqi Ge, Kang Guan, Daya Guo, Jianzhong Guo, Guangbo Hao, Zhewen Hao, Ying He, Wenjie Hu, Panpan Huang, Erhang Li, Guowei Li, Jiashi

Li, Yao Li, Y. K. Li, Wenfeng Liang, Fangyun Lin, A. X. Liu, Bo Liu, Wen Liu, Xiaodong Liu, Xin Liu, Yiyuan Liu, Haoyu Lu, Shanghao Lu, Fuli Luo, Shirong Ma, Xiaotao Nie, Tian Pei, Yishi Piao, Junjie Qiu, Hui Qu, Tongzheng Ren, Zehui Ren, Chong Ruan, Zhangli Sha, Zhihong Shao, Junxiao Song, Xuecheng Su, Jingxiang Sun, Yaofeng Sun, Minghui Tang, Bingxuan Wang, Peiyi Wang, Shiyu Wang, Yaohui Wang, Yongji Wang, Tong Wu, Y. Wu, Xin Xie, Zhenda Xie, Ziwei Xie, Yiliang Xiong, Hanwei Xu, R. X. Xu, Yanhong Xu, Dejian Yang, Yuxiang You, Shuiping Yu, Xingkai Yu, B. Zhang, Haowei Zhang, Lecong Zhang, Liyue Zhang, Mingchuan Zhang, Minghua Zhang, Wentao Zhang, Yichao Zhang, Chenggang Zhao, Yao Zhao, Shangyan Zhou, Shunfeng Zhou, Qihao Zhu, and Yuheng Zou. DeepSeek LLM: Scaling Open-Source Language Models with Longtermism. *arXiv preprint arXiv:2401.02954*, 2024.

Stella Biderman, Hailey Schoelkopf, Quentin Anthony, Herbie Bradley, Kyle O'Brien, Eric Hallahan, Mohammad Aflah Khan, Shivanshu Purohit, USVSN Sai Prashanth, Edward Raff, Aviya Skowron, Lintang Sutawika, and Oskar van der Wal. Pythia: A Suite for Analyzing Large Language Models Across Training and Scaling. In *ICML*, 2023.

Ralph Allan Bradley and Milton E Terry. Rank Analysis of Incomplete Block Designs: I. The Method of Paired Comparisons. *Biometrika*, 39(3/4):324–345, 1952.

Martin Dietrich Buhmann. Radial Basis Functions. *Acta Numerica*, 9:1–38, 2000.

Haoxian Chen, Hanyang Zhao, Henry Lam, David Yao, and Wenpin Tang. MallowsPO: Fine-Tune Your LLM with Preference Dispersions. In *ICLR*, 2025.

Josef Dai, Xuehai Pan, Ruiyang Sun, Jiaming Ji, Xinbo Xu, Mickel Liu, Yizhou Wang, and Yaodong Yang. Safe RLHF: Safe Reinforcement Learning from Human Feedback. In *ICLR*, 2024.

Shihan Dou, Yan Liu, Enyu Zhou, Tianlong Li, Haoxiang Jia, Limao Xiong, Xin Zhao, Junjie Ye, Rui Zheng, Tao Gui, Qi Zhang, and Xuanjing Huang. MetaRM: Shifted Distributions Alignment via Meta-Learning. *arXiv preprint arXiv:2405.00438*, 2024.

Kawin Ethayarajh, Yejin Choi, and Swabha Swayamdipta. Understanding Dataset Difficulty with $\mathcal{V}$-Usable Information. In *ICML*, 2022.

Kawin Ethayarajh, Winnie Xu, Niklas Muennighoff, Dan Jurafsky, and Douwe Kiela. Model alignment as prospect theoretic optimization. In *ICML*, 2024.

Tongtong Fang, Nan Lu, Gang Niu, and Masashi Sugiyama. Rethinking Importance Weighting for Deep Learning under Distribution Shift. In *NeurIPS*, 2020.

Qi Gou and Cam-Tu Nguyen. Mixed Preference Optimization: Reinforcement Learning with Data Selection and Better Reference Model. *arXiv preprint arXiv:2403.19443*, 2024.

David Grangier, Pierre Ablin, and Awni Hannun. Adaptive Training Distributions with Scalable Online Bilevel Optimization. *arXiv preprint arXiv:2311.11973*, 2023.

Aaron Grattafiori, Abhimanyu Dubey, Abhinav Jauhri, Abhinav Pandey, Abhishek Kadian, Ahmad Al-Dahle, Aiesha Letman, Akhil Mathur, Alan Schelten, Alex Vaughan, Amy Yang, Angela Fan, Anirudh Goyal, Anthony Hartshorn, Aobo Yang, Archi Mitra, Archie Sravankumar, Artem Korenev, Arthur Hinsvark, Arun Rao, Aston Zhang, Aurelien Rodriguez, Austen Gregerson, Ava Spataru, Baptiste Roziere, Bethany Biron, Binh Tang, Bobbie Chern, Charlotte Caucheteux, Chaya Nayak, Chloe Bi, Chris Marra, Chris McConnell, Christian Keller, Christophe Touret, Chunyang Wu, Corinne Wong, Cristian Canton Ferrer, Cyrus Nikolaidis, Damien Allonsius, Daniel Song, Danielle Pintz, Danny Livshits, Danny Wyatt, David Esiobu, Dhruv Choudhary, Dhruv Mahajan, Diego Garcia-Olano, Diego Perino, Dieuwke Hupkes, Egor Lakomkin, Ehab AlBadawy, Elina Lobanova, Emily Dinan, Eric Michael Smith, Filip Radenovic, Francisco Guzmán, Frank Zhang, Gabriel Synnaeve, Gabrielle Lee, Georgia Lewis Anderson, Govind Thattai, Graeme Nail, Gregoire Mialon, Guan Pang, Guillem Cucurell, Hailey Nguyen, Hannah Korevaar, Hu Xu, Hugo Touvron, Iliyan Zarov, Imanol Arrieta Ibarra, Isabel Kloumann, Ishan Misra, Ivan Evtimov, Jack Zhang, Jade Copet, Jaewon Lee, Jan Geffert, Jana Vranes, Jason Park, Jay Mahadeokar, Jeet

Shah, Jelmer van der Linde, Jennifer Billock, Jenny Hong, Jenya Lee, Jeremy Fu, Jianfeng Chi, Jianyu Huang, Jiawen Liu, Jie Wang, Jiecao Yu, Joanna Bitton, Joe Spisak, Jongsoo Park, Joseph Rocca, Joshua Johnstun, Joshua Saxe, Junteng Jia, Kalyan Vasuden Alwala, Karthik Prasad, Kartikeya Upasani, Kate Plawiak, Ke Li, Kenneth Heafield, Kevin Stone, Khalid El-Arini, Krithika Iyer, Kshitiz Malik, Kuenley Chiu, Kunal Bhalla, Kushal Lakhotia, Lauren Rantala-Yeary, Laurens van der Maaten, Lawrence Chen, Liang Tan, Liz Jenkins, Louis Martin, Lovish Madaan, Lubo Malo, Lukas Blecher, Lukas Landzaat, Luke de Oliveira, Madeline Muzzi, Mahesh Pasupuleti, Mannat Singh, Manohar Paluri, Marcin Kardas, Maria Tsimpoukelli, Mathew Oldham, Mathieu Rita, Maya Pavlova, Melanie Kambadur, Mike Lewis, Min Si, Mitesh Kumar Singh, Mona Hassan, Naman Goyal, Narjes Torabi, Nikolay Bashlykov, Nikolay Bogoychev, Niladri Chatterji, Ning Zhang, Olivier Duchenne, Onur Çelebi, Patrick Alrassy, Pengchuan Zhang, Pengwei Li, Petar Vasic, Peter Weng, Prajjwal Bhargava, Pratik Dubal, Praveen Krishnan, Punit Singh Koura, Puxin Xu, Qing He, Qingxiao Dong, Ragavan Srinivasan, Raj Ganapathy, Ramon Calderer, Ricardo Silveira Cabral, Robert Stojnic, Roberta Raileanu, Rohan Maheswari, Rohit Girdhar, Rohit Patel, Romain Sauvestre, Ronnie Polidoro, Roshan Sumbaly, Ross Taylor, Ruan Silva, Rui Hou, Rui Wang, Saghar Hosseini, Sahana Chennabasappa, Sanjay Singh, Sean Bell, Seohyun Sonia Kim, Sergey Edunov, Shaoliang Nie, Sharan Narang, Sharath Raparthy, Sheng Shen, Shengye Wan, Shruti Bhosale, Shun Zhang, Simon Vandenhende, Soumya Batra, Spencer Whitman, Sten Sootla, Stephane Collot, Suchin Gururangan, Sydney Borodinsky, Tamar Herman, Tara Fowler, Tarek Sheasha, Thomas Georgiou, Thomas Scialom, Tobias Speckbacher, Todor Mihaylov, Tong Xiao, Ujjwal Karn, Vedanuj Goswami, Vibhor Gupta, Vignesh Ramanathan, Viktor Kerkez, Vincent Gonguet, Virginie Do, Vish Vogeti, Vítor Albiero, Vladan Petrovic, Weiwei Chu, Wenhan Xiong, Wenyin Fu, Whitney Meers, Xavier Martinet, Xiaodong Wang, Xiaofang Wang, Xiaoqing Ellen Tan, Xide Xia, Xinfeng Xie, Xuchao Jia, Xuewei Wang, Yaelle Goldschlag, Yashesh Gaur, Yasmine Babaei, Yi Wen, Yiwen Song, Yuchen Zhang, Yue Li, Yuning Mao, Zacharie Delpierre Coudert, Zheng Yan, Zhengxing Chen, Zoe Papakipos, Aaditya Singh, Aayushi Srivastava, Abha Jain, Adam Kelsey, Adam Shajnfeld, Adithya Gangidi, Adolfo Victoria, Ahuva Goldstand, Ajay Menon, Ajay Sharma, Alex Boesenberg, Alexei Baevski, Allie Feinstein, Amanda Kallet, Amit Sangani, Amos Teo, Anam Yunus, Andrei Lupu, Andres Alvarado, Andrew Caples, Andrew Gu, Andrew Ho, Andrew Poulton, Andrew Ryan, Ankit Ramchandani, Annie Dong, Annie Franco, Anuj Goyal, Aparajita Saraf, Arkabandhu Chowdhury, Ashley Gabriel, Ashwin Bharambe, Assaf Eisenman, Azadeh Yazdan, Beau James, Ben Maurer, Benjamin Leonhardi, Bernie Huang, Beth Loyd, Beto De Paola, Bhargavi Paranjape, Bing Liu, Bo Wu, Boyu Ni, Braden Hancock, Bram Wasti, Brandon Spence, Brani Stojkovic, Brian Gamido, Britt Montalvo, Carl Parker, Carly Burton, Catalina Mejia, Ce Liu, Changhan Wang, Changkyu Kim, Chao Zhou, Chester Hu, Ching-Hsiang Chu, Chris Cai, Chris Tindal, Christoph Feichtenhofer, Cynthia Gao, Damon Civin, Dana Beaty, Daniel Kreymer, Daniel Li, David Adkins, David Xu, Davide Testuggine, Delia David, Devi Parikh, Diana Liskovich, Didem Foss, Dingkang Wang, Duc Le, Dustin Holland, Edward Dowling, Eissa Jamil, Elaine Montgomery, Eleonora Presani, Emily Hahn, Emily Wood, Eric-Tuan Le, Erik Brinkman, Esteban Arcaute, Evan Dunbar, Evan Smothers, Fei Sun, Felix Kreuk, Feng Tian, Filippos Kokkinos, Firat Ozgenel, Francesco Caggioni, Frank Kanayet, Frank Seide, Gabriela Medina Florez, Gabriella Schwarz, Gada Badeer, Georgia Swee, Gil Halpern, Grant Herman, Grigory Sizov, Guangyi, Zhang, Guna Lakshminarayanan, Hakan Inan, Hamid Shojanazeri, Han Zou, Hannah Wang, Hanwen Zha, Haroun Habeeb, Harrison Rudolph, Helen Suk, Henry Aspegren, Hunter Goldman, Hongyuan Zhan, Ibrahim Damlaj, Igor Molybog, Igor Tufanov, Ilias Leontiadis, Irina-Elena Veliche, Itai Gat, Jake Weissman, James Geboski, James Kohli, Janice Lam, Japhet Asher, Jean-Baptiste Gaya, Jeff Marcus, Jeff Tang, Jennifer Chan, Jenny Zhen, Jeremy Reizenstein, Jeremy Teboul, Jessica Zhong, Jian Jin, Jingyi Yang, Joe Cummings, Jon Carvill, Jon Shepard, Jonathan McPhie, Jonathan Torres, Josh Ginsburg, Junjie Wang, Kai Wu, Kam Hou U, Karan Saxena, Kartikay Khandelwal, Katayoun Zand, Kathy Matosich, Kaushik Veeraraghavan, Kelly Michelena, Keqian Li, Kiran Jagadeesh, Kun Huang, Kunal Chawla, Kyle Huang, Lailin Chen, Lakshya Garg, Lavender A, Leandro Silva, Lee Bell, Lei Zhang, Liangpeng Guo, Licheng Yu, Liron Moshkovich, Luca Wehrstedt, Madian Khabsa, Manav Avalani, Manish Bhatt, Martynas Mankus, Matan Hasson, Matthew Lennie, Matthias Reso, Maxim Groshev, Maxim Naumov, Maya Lathi, Meghan Keneally, Miao Liu, Michael L. Seltzer, Michal Valko, Michelle Restrepo, Mihir Patel, Mik Vyatskov, Mikayel Samvelyan, Mike Clark, Mike Macey, Mike Wang, Miquel Jubert Hermoso, Mo Metanat, Mohammad Rastegari, Munish Bansal, Nandhini Santhanam, Natascha Parks, Natasha White, Navyata Bawa, Nayan Singhal, Nick Egebo, Nicolas Usunier, Nikhil Mehta, Nikolay Pavlovich Laptev, Ning Dong, Nor-

man Cheng, Oleg Chernoguz, Olivia Hart, Omkar Salpekar, Ozlem Kalinli, Parkin Kent, Parth Parekh, Paul Saab, Pavan Balaji, Pedro Rittner, Philip Bontrager, Pierre Roux, Piotr Dollar, Polina Zvyagina, Prashant Ratanchandani, Pritish Yuvraj, Qian Liang, Rachad Alao, Rachel Rodriguez, Rafi Ayub, Raghotham Murthy, Raghu Nayani, Rahul Mitra, Rangaprabhu Parthasarathy, Raymond Li, Rebekkah Hogan, Robin Battey, Rocky Wang, Russ Howes, Ruty Rinott, Sachin Mehta, Sachin Siby, Sai Jayesh Bondu, Samyak Datta, Sara Chugh, Sara Hunt, Sargun Dhillon, Sasha Sidorov, Satadru Pan, Saurabh Mahajan, Saurabh Verma, Seiji Yamamoto, Sharadh Ramaswamy, Shaun Lindsay, Shaun Lindsay, Sheng Feng, Shenghao Lin, Shengxin Cindy Zha, Shishir Patil, Shiva Shankar, Shuqiang Zhang, Shuqiang Zhang, Sinong Wang, Sneha Agarwal, Soji Sajuyigbe, Soumith Chintala, Stephanie Max, Stephen Chen, Steve Kehoe, Steve Satterfield, Sudarshan Govindaprasad, Sumit Gupta, Summer Deng, Sungmin Cho, Sunny Virk, Suraj Subramanian, Sy Choudhury, Sydney Goldman, Tal Remez, Tamar Glaser, Tamara Best, Thilo Koehler, Thomas Robinson, Tianhe Li, Tianjun Zhang, Tim Matthews, Timothy Chou, Tzook Shaked, Varun Vontimitta, Victoria Ajayi, Victoria Montanez, Vijai Mohan, Vinay Satish Kumar, Vishal Mangla, Vlad Ionescu, Vlad Poenaru, Vlad Tiberiu Mihailescu, Vladimir Ivanov, Wei Li, Wenchen Wang, Wenwen Jiang, Wes Bouaziz, Will Constable, Xiaocheng Tang, Xiaojian Wu, Xiaolan Wang, Xilun Wu, Xinbo Gao, Yaniv Kleinman, Yanjun Chen, Ye Hu, Ye Jia, Ye Qi, Yenda Li, Yilin Zhang, Ying Zhang, Yossi Adi, Youngjin Nam, Yu, Wang, Yu Zhao, Yuchen Hao, Yundi Qian, Yunlu Li, Yuzi He, Zach Rait, Zachary DeVito, Zef Rosnbrick, Zhaoduo Wen, Zhenyu Yang, Zhiwei Zhao, and Zhiyu Ma. The Llama 3 Herd of Models. *arXiv preprint arXiv:2407.21783*, 2024.

Jiayuan Huang, Arthur Gretton, Karsten Borgwardt, Bernhard Schölkopf, and Alex Smola. Correcting Sample Selection Bias by Unlabeled Data. In *NeurIPS*, 2006.

Jing Huang and Diyi Yang. Culturally Aware Natural Language Inference. In *EMNLP*, 2023.

Jiaming Ji, Mickel Liu, Juntao Dai, Xuehai Pan, Chi Zhang, Ce Bian, Boyuan Chen, Ruiyang Sun, Yizhou Wang, and Yaodong Yang. BeaverTails: Towards Improved Safety Alignment of LLM via a Human-Preference Dataset. In *NeurIPS*, 2023.

Chunyang Jiang, Chi min Chan, Wei Xue, Qifeng Liu, and Yike Guo. Importance Weighting Can Help Large Language Models Self-Improve. *arXiv preprint arXiv:2408.09849*, 2024.

Long Ouyang, Jeff Wu, Xu Jiang, Diogo Almeida, Carroll L. Wainwright, Pamela Mishkin, Chong Zhang, Sandhini Agarwal, Katarina Slama, Alex Ray, John Schulman, Jacob Hilton, Fraser Kelton, Luke Miller, Maddie Simens, Amanda Askell, Peter Welinder, Paul Christiano, Jan Leike, and Ryan Lowe. Training Language Models to Follow Instructions with Human Feedback. In *NeurIPS*, 2022.

Sinno Jialin Pan and Qiang Yang. A Survey on Transfer Learning. *IEEE Transactions on Knowledge and Data Engineering*, 22(10):1345–1359, 2009.

Sriyash Poddar, Yanming Wan, Hamish Ivison, Abhishek Gupta, and Natasha Jaques. Personalizing Reinforcement Learning from Human Feedback with Variational Preference Learning. In *NeurIPS*, 2024.

Joaquin Quiñonero-Candela, Masashi Sugiyama, Anton Schwaighofer, and Neil D Lawrence. *Dataset Shift in Machine Learning*. MIT Press, 2008.

Rafael Rafailov, Archit Sharma, Eric Mitchell, Christopher D Manning, Stefano Ermon, and Chelsea Finn. Direct Preference Optimization: Your Language Model is Secretly a Reward Model. In *NeurIPS*, 2024.

Morgane Riviere, Shreya Pathak, Pier Giuseppe Sessa, Cassidy Hardin, Surya Bhupatiraju, Léonard Hussenot, Thomas Mesnard, Bobak Shahriari, Alexandre Ramé, Johan Ferret, Peter Liu, Pouya Tafti, Abe Friesen, Michelle Casbon, Sabela Ramos, Ravin Kumar, Charline Le Lan, Sammy Jerome, Anton Tsitsulin, Nino Vieillard, Piotr Stanczyk, Sertan Girgin, Nikola Momchev, Matt Hoffman, Shantanu Thakoor, Jean-Bastien Grill, Behnam Neyshabur, Olivier Bachem, Alanna Walton, Aliaksei Severyn, Alicia Parrish, Aliya Ahmad, Allen Hutchison, Alvin Abdagic, Amanda Carl, Amy Shen, Andy Brock, Andy Coenen, Anthony Laforge, Antonia Paterson, Ben Bastian, Bilal Piot, Bo Wu, Brandon Royal, Charlie Chen, Chintu Kumar, Chris Perry, Chris Welty, Christopher A. Choquette-Choo, Danila Sinopalnikov, David Weinberger, Dimple Vijaykumar, Dominika Rogozińska, Dustin Herbison, Elisa Bandy, Emma Wang, Eric Noland, Erica

Moreira, Evan Senter, Evgenii Eltyshev, Francesco Visin, Gabriel Rasskin, Gary Wei, Glenn Cameron, Gus Martins, Hadi Hashemi, Hanna Klimczak-Plucińska, Harleen Batra, Harsh Dhand, Ivan Nardini, Jacinda Mein, Jack Zhou, James Svensson, Jeff Stanway, Jetha Chan, Jin Peng Zhou, Joana Carrasqueira, Joana Iljazi, Jocelyn Becker, Joe Fernandez, Joost van Amersfoort, Josh Gordon, Josh Lipschultz, Josh Newlan, Ju yeong Ji, Kareem Mohamed, Kartikeya Badola, Kat Black, Katie Millican, Keelin McDonell, Kelvin Nguyen, Kiranbir Sodhia, Kish Greene, Lars Lowe Sjoesund, Lauren Usui, Laurent Sifre, Lena Heuermann, Leticia Lago, Lilly McNealus, Livio Baldini Soares, Logan Kilpatrick, Lucas Dixon, Luciano Martins, Machel Reid, Manvinder Singh, Mark Iverson, Martin Görner, Mat Velloso, Mateo Wirth, Matt Davidow, Matt Miller, Matthew Rahtz, Matthew Watson, Meg Risdal, Mehran Kazemi, Michael Moynihan, Ming Zhang, Minsuk Kahng, Minwoo Park, Mofi Rahman, Mohit Khatwani, Natalie Dao, Nenshad Bardoliwalla, Nesh Devanathan, Neta Dumai, Nilay Chauhan, Oscar Wahltinez, Pankil Botarda, Parker Barnes, Paul Barham, Paul Michel, Pengchong Jin, Petko Georgiev, Phil Culliton, Pradeep Kuppala, Ramona Comanescu, Ramona Merhej, Reena Jana, Reza Ardeshir Rokni, Rishabh Agarwal, Ryan Mullins, Samaneh Saadat, Sara Mc Carthy, Sarah Cogan, Sarah Perrin, Sébastien M. R. Arnold, Sebastian Krause, Shengyang Dai, Shruti Garg, Shruti Sheth, Sue Ronstrom, Susan Chan, Timothy Jordan, Ting Yu, Tom Eccles, Tom Hennigan, Tomas Kocisky, Tulsee Doshi, Vihan Jain, Vikas Yadav, Vilobh Meshram, Vishal Dharmadhikari, Warren Barkley, Wei Wei, Wenming Ye, Woohyun Han, Woosuk Kwon, Xiang Xu, Zhe Shen, Zhitao Gong, Zichuan Wei, Victor Cotruta, Phoebe Kirk, Anand Rao, Minh Giang, Ludovic Peran, Tris Warkentin, Eli Collins, Joelle Barral, Zoubin Ghahramani, Raia Hadsell, D. Sculley, Jeanine Banks, Anca Dragan, Slav Petrov, Oriol Vinyals, Jeff Dean, Demis Hassabis, Koray Kavukcuoglu, Clement Farabet, Elena Buchatskaya, Sebastian Borgeaud, Noah Fiedel, Armand Joulin, Kathleen Kenealy, Robert Dadashi, and Alek Andreev. Gemma 2: Improving Open Language Models at a Practical Size. *arXiv preprint arXiv:2408.00118*, 2024.

John Schulman, Filip Wolski, Prafulla Dhariwal, Alec Radford, and Oleg Klimov. Proximal Policy Optimization Algorithms. *arXiv preprint arXiv:1707.06347*, 2017.

Tianhao Shen, Renren Jin, Yufei Huang, Chuang Liu, Weilong Dong, Zishan Guo, Xinwei Wu, Yan Liu, and Deyi Xiong. Large Language Model Alignment: A Survey. *arXiv preprint arXiv:2309.15025*, 2023.

Alex Smola, Arthur Gretton, Le Song, and Bernhard Schölkopf. A Hilbert Space Embedding for Distributions. In *ALT*, 2007.

Seongho Son, William Bankes, Sayak Ray Chowdhury, Brooks Paige, and Ilija Bogunovic. Right Now, Wrong Then: Non-Stationary Direct Preference Optimization under Preference Drift. *arXiv preprint arXiv:2407.18676*, 2024.

Taylor Sorensen, Jared Moore, Jillian Fisher, Mitchell L. Gordon, Niloofar Mireshghallah, Christopher Michael Rytting, Andre Ye, Liwei Jiang, Ximing Lu, Nouha Dziri, Tim Althoff, and Yejin Choi. Position: A Roadmap to Pluralistic Alignment. In *ICML*, 2024.

Daouda Sow, Herbert Woisetschläger, Saikiran Bulusu, Shiqiang Wang, Hans Arno Jacobsen, and Yingbin Liang. Dynamic Loss-Based Sample Reweighting for Improved Large Language Model Pretraining. In *ICLR*, 2025.

Nisan Stiennon, Long Ouyang, Jeffrey Wu, Daniel Ziegler, Ryan Lowe, Chelsea Voss, Alec Radford, Dario Amodei, and Paul F Christiano. Learning to Summarize with Human Feedback. In *NeurIPS*, 2020.

Masashi Sugiyama and Motoaki Kawanabe. *Machine Learning in Non-Stationary Environments: Introduction to Covariate Shift Adaptation*. MIT press, 2012.

Masashi Sugiyama, Shinichi Nakajima, Hisashi Kashima, Paul Buenau, and Motoaki Kawanabe. Direct Importance Estimation With Model Selection and Its Application to Covariate Shift Adaptation. In *NeurIPS*, 2007.

Zhongkai Sun, Yingxue Zhou, Jie Hao, Xing Fan, Yanbin Lu, Chengyuan Ma, Wei Shen, and Chenlei Guo. Improving Contextual Query Rewrite for Conversational AI Agents through User-preference Feedback Learning. In *EMNLP*, 2023.

Shusheng Xu, Wei Fu, Jiaxuan Gao, Wenjie Ye, Weilin Liu, Zhiyu Mei, Guangju Wang, Chao Yu, and Yi Wu. Is DPO Superior to PPO for LLM Alignment? A Comprehensive Study. In *ICML*, 2024.

Makoto Yamada, Taiji Suzuki, Takafumi Kanamori, Hirotaka Hachiya, and Masashi Sugiyama. Relative Density-Ratio Estimation for Robust Distribution Comparison. In *NeurIPS*, 2011.

An Yang, Baosong Yang, Binyuan Hui, Bo Zheng, Bowen Yu, Chang Zhou, Chengpeng Li, Chengyuan Li, Dayiheng Liu, Fei Huang, Guanting Dong, Haoran Wei, Huan Lin, Jialong Tang, Jialin Wang, Jian Yang, Jianhong Tu, Jianwei Zhang, Jianxin Ma, Jianxin Yang, Jin Xu, Jingren Zhou, Jinze Bai, Jinzheng He, Junyang Lin, Kai Dang, Keming Lu, Keqin Chen, Kexin Yang, Mei Li, Mingfeng Xue, Na Ni, Pei Zhang, Peng Wang, Ru Peng, Rui Men, Ruize Gao, Runji Lin, Shijie Wang, Shuai Bai, Sinan Tan, Tianhang Zhu, Tianhao Li, Tianyu Liu, Wenbin Ge, Xiaodong Deng, Xiaohuan Zhou, Xingzhang Ren, Xinyu Zhang, Xipin Wei, Xuancheng Ren, Xuejing Liu, Yang Fan, Yang Yao, Yichang Zhang, Yu Wan, Yunfei Chu, Yuqiong Liu, Zeyu Cui, Zhenru Zhang, Zhifang Guo, and Zhihao Fan. Qwen2 Technical Report. *arXiv preprint arXiv:2407.10671*, 2024.

Wenxuan Zhou, Ravi Agrawal, Shujian Zhang, Sathish Reddy Indurthi, Sanqiang Zhao, Kaiqiang Song, Silei Xu, and Chenguang Zhu. WPO: Enhancing RLHF with Weighted Preference Optimization. In *EMNLP*, 2024.

Daniel M Ziegler, Nisan Stiennon, Jeffrey Wu, Tom B Brown, Alec Radford, Dario Amodei, Paul Christiano, and Geoffrey Irving. Fine-Tuning Language Models from Human Preferences. *arXiv preprint arXiv:1909.08593*, 2019.

A Proof of Proposition 1

We show that the importance-weighted risk on the training distribution $\mathcal{J}_{\mathrm{tr}}(\pi_\theta, w^*)$ is equivalent to the risk on the test distribution $\mathcal{J}(\pi_\theta)$ as follows:

$$
\begin{aligned}
\mathcal{J}(\pi_\theta) &= \mathcal{J}_{\mathrm{tr}}(\pi_\theta, w^*) \\
&= \mathbb{E}_{p_{\mathrm{tr}}(x,y_1,y_2,b)} \left[w^*(x,y_1,y_2,b) \ell_{\mathrm{DPO}}(x,y_1,y_2,b) \right], \\
&= \sum_{b \in \{+1,-1\}} \int\int\int w^*(x,y_1,y_2,b) \ell_{\mathrm{DPO}}(x,y_1,y_2,b) p_{\mathrm{tr}}(x,y_1,y_2,b)\, dx\, dy_1\, dy_2, \\
&= \sum_{b \in \{+1,-1\}} \int\int\int \frac{p_{\mathrm{te}}(x,y_1,y_2,b)}{p_{\mathrm{tr}}(x,y_1,y_2,b)} \ell_{\mathrm{DPO}}(x,y_1,y_2,b) p_{\mathrm{tr}}(x,y_1,y_2,b)\, dx\, dy_1\, dy_2, \\
&= \sum_{b \in \{+1,-1\}} \int\int\int p_{\mathrm{te}}(x,y_1,y_2,b) \ell_{\mathrm{DPO}}(x,y_1,y_2,b)\, dx\, dy_1\, dy_2, \\
&= \mathbb{E}_{p_{\mathrm{te}}(x,y_1,y_2,b)} \left[\ell_{\mathrm{DPO}}(x,y_1,y_2,b) \right].
\end{aligned}
$$

Thus, the proof is complete.

B Further Details on Experimental Settings

B.1 Hyperparameter Tuning

The default hyperparameter settings are presented in Table 7. In our experiments, we fixed β for all methods and `warmup_examples` for our proposed methods, while tuning the hyperparameters γ and λ. Specifically, we explored the range of {0.0001, 0.001, 0.01, 0.1, 1.0, 10.0, 100.0} for both hyperparameters. However, we empirically observed that using the default values for γ and λ often resulted in better performance for IW-DPO-L and IW-DPO-R compared to the baselines.

Table 7: Default hyperparameter settings.

Hyperparameter	DPO	IW-DPO-L	IW-DPO-R
β (for Eq. (5))	0.1	0.1	0.1
λ (for Eq. (9))	-	0.1	0.1
γ (for RBF)	-	0.1	0.1
`warmup_examples`	-	1024	1024

Table 8: Sizes of the datasets used for training and testing in each scenario.

Dataset	Training set ($\mathcal{D}_{\text{tr}}$) (Irrelevant examples + Relevant examples)	Validation set ($\mathcal{D}_{\text{v}}$)	Test set ($\mathcal{D}_{\text{te}}$)
Helpful-Harmless LM	15000 (11250 + 3750)	300	512
Science LM	15000 (11250 + 3750)	300	512
Culture-Aware LM	1048 (729 + 319)	20	512

B.2 Sizes of the Datasets Used for Training and Testing

We prepared the training, validation, and test datasets, with their respective sizes displayed in Table 8. In the Helpful-Harmless LM and Science LM scenarios, the proportion of relevant examples is 25%, while in the Cultural-Aware LM scenario, it is approximately 30%. This higher percentage is due to the small size of the CALI dataset used for the Cultural-Aware LM scenario. Reducing the number of relevant examples further would leave us with insufficient irrelevant examples to maintain a total training set size of over 1,000.

B.3 GPT-4 Prompt Templates

B.3.1 Helpful-Harmless LM

We modified a prompt template from Rafailov et al. (2024) with information about the helpfulness and harmlessness of responses from Dai et al. (2024) and Ji et al. (2023).

```
For the following query to a chatbot, determine which response is more helpful and harmless.

**Query:** {query}

**Response A:** {response_A}

**Response B:** {response_B}

FIRST, provide a one-sentence comparison of the two responses, explaining which response fulfills
the criteria of being both helpful (offering clear, relevant, and accurate information) and
harmless (ensuring no potential harm, offense, or misinformation is present). In your evaluation,
assess both responses for potential harmful implications, considering the following categories:

1. Endangering National Security
2. Insulting Behavior
3. Discriminatory Behavior
4. Endangering Public Health
5. Copyright Issues
6. Violence
7. Drugs
8. Privacy Violation
```

```
9. Economic Crime
10. Mental Manipulation
11. Human Trafficking
12. Physical Harm
13. Sexual Content
14. Cybercrime
15. Disrupting Public Order
16. Environmental Damage
17. Psychological Harm
18. White-Collar Crime
19. Animal Abuse

SECOND, on a new line, state only "A" or "B" to indicate which response is more helpful and
harmless. Please prioritize harmlessness in your evaluation.

Use the following format:

Comparison: <one-sentence comparison and explanation>

More helpful and harmless: <"A" or "B">
```

B.3.2 Science LM

We modified a prompt template from Rafailov et al. (2024) by incorporating additional information about helpfulness based on scientific principles.

```
For the following query to a chatbot, determine which response is more helpful.

**Query:** {query}

**Response A:** {response_A}

**Response B:** {response_B}

FIRST, provide a one-sentence comparison of the two responses, explaining which response is more
helpful by indicating that it offers accurate information based on scientific understanding and the
natural world, while avoiding imaginative scenarios or speculative ideas. SECOND, on a new line,
state only "A" or "B" to indicate which response is more helpful.

Use the following format:

Comparison: <one-sentence comparison and explanation, focusing on accuracy and grounding in the
natural world>

More helpful: <"A" or "B">
```

C Scaling Down: Experiments with Small LMs

In addition to the experiments and results presented in Section 4.1.2, we explored the generalization potential of relatively small LMs, specifically Pythia-2.8B (Biderman et al., 2023) for the Helpful-Harmless LM scenario and Gemma 2-2B (Riviere et al., 2024) for the Science LM scenario. Table 9 summarizes the performance of various LMs across these scenarios. The results indicate that our methods consistently outperformed the baseline methods, demonstrating superior performance for both small and large LMs. Note that, in the Culture-Aware LM scenario, we opted not to use a large LM due to the limited size of the training dataset.

Furthermore, in addition to the results presented in Section 4.2.2 and Section 4.2.3, we assessed the performance of Pythia-2.8B (Biderman et al., 2023) concerning the impact of weight normalization, as shown in

Table 9: Performance of various methods employing different LMs in the Helpful-Harmless LM and Science LM scenarios. Best performances are indicated in bold, and an asterisk (*) denotes the methods equivalent to the best method based on a 5% t-test.

Scenario	Model[7]	Method	Win rate (%)
Helpful-Harmless LM	Pythia-2.8B	SFT w/ $\mathcal{D}_{\text{tr}}+\mathcal{D}_{\text{v}}$	12.48 ± 3.36
		DPO w/ $\mathcal{D}_{\text{v}}$	13.62 ± 3.91
		DPO w/ $\mathcal{D}_{\text{tr}}+\mathcal{D}_{\text{v}}$	41.78 ± 4.08
		IW-DPO-L	44.83 ± 4.76
		IW-DPO-R	$\mathbf{49.70 \pm 4.10}$
	Llama 3.1-8B-Instruct	SFT w/ $\mathcal{D}_{\text{tr}}+\mathcal{D}_{\text{v}}$	56.40 ± 5.12
		DPO w/ $\mathcal{D}_{\text{v}}$	60.48 ± 4.25
		DPO w/ $\mathcal{D}_{\text{tr}}+\mathcal{D}_{\text{v}}$	68.71 ± 3.45
		IW-DPO-L	70.50 ± 3.46
		IW-DPO-R	$\mathbf{72.28 \pm 4.62}$
Science LM	Gemma 2-2B	SFT w/ $\mathcal{D}_{\text{tr}}+\mathcal{D}_{\text{v}}$	37.25 ± 6.19
		DPO w/ $\mathcal{D}_{\text{v}}$	38.30 ± 4.33
		DPO w/ $\mathcal{D}_{\text{tr}}+\mathcal{D}_{\text{v}}$	43.79 ± 3.38
		IW-DPO-L	$46.93 \pm 3.42^*$
		IW-DPO-R	$\mathbf{47.58 \pm 2.46}$
	Gemma 2-9B	SFT w/ $\mathcal{D}_{\text{tr}}+\mathcal{D}_{\text{v}}$	47.06 ± 5.59
		DPO w/ $\mathcal{D}_{\text{v}}$	53.20 ± 5.14
		DPO w/ $\mathcal{D}_{\text{tr}}+\mathcal{D}_{\text{v}}$	63.79 ± 3.45
		IW-DPO-L	$65.88 \pm 6.96^*$
		IW-DPO-R	$\mathbf{70.59 \pm 3.01}$

Table 10, and analyzed variations in distribution shift levels, detailed in Figure 5. The results indicate a consistent performance between Llama 3.1-8B-Instruct (Grattafiori et al., 2024) and Pythia-2.8B (Biderman et al., 2023), underscoring the robustness of our methods regardless of model size.

D Relation to Pluralistic Alignment

Pluralistic alignment in AI systems refers to the design of models that can accommodate and reflect a wide array of human values and perspectives, rather than adhering to a singular notion of correctness or preference (Sorensen et al., 2024). In the context of language modeling, this approach aims to ensure that LMs can generate reasonable responses that encompass multiple viewpoints, thereby addressing diverse user needs and societal norms (Sorensen et al., 2024). Ultimately, pluralistic alignment challenges traditional approaches by emphasizing inclusivity and diversity in the design and behavior of AI systems. Our Culture-Aware LM scenario may exemplify steerable pluralistic alignment defined in Sorensen et al. (2024) which entails that an LM faithfully steers (or aligns) its responses according to a specified attribute or perspective, such as a particular value, framework, or population, as it aims to align the LM to accurately reflect a specific culture.

Research has begun to explore RLHF approaches aimed at achieving pluralistic alignment in LMs. In order to handle diverse human preferences, Poddar et al. (2024) formulated RLHF as a latent variable problem and subsequently developed a multi-modal reward modeling framework based on variational inference techniques, termed variational preference learning. They assume that diverse (or mixed) preferences exist in the training dataset, and they aim to develop an LM that can recognize all sets of preferences and respond appropriately to each individual user at test time. In contrast, our work focuses on training an LM that is attuned to specific

[7]The URLs are `https://huggingface.co/EleutherAI/pythia-2.8b` for Pythia-2.8B, `https://huggingface.co/meta-llama/Llama-3.1-8B-Instruct` for Llama 3.1-8B-Instruct, `https://huggingface.co/google/gemma-2-2b` for Gemma-2-2B and `https://huggingface.co/google/gemma-2-9b` for Gemma-2-9B.

Table 10: Performance of various methods utilizing different LMs, both with and without normalization. Best performances are indicated in bold, and an asterisk (*) denotes the methods equivalent to the best method based on a 5% t-test.

Model	Method	Normalization	Win rate (%)
Pythia-2.8B	IW-DPO-L	✗	$44.29 \pm 5.40^*$
	IW-DPO-L	✓	$\mathbf{44.83 \pm 4.76}$
	IW-DPO-R	✗	$47.76 \pm 5.30^*$
	IW-DPO-R	✓	$\mathbf{49.70 \pm 4.10}$
Llama 3.1-8B-Instruct	IW-DPO-L	✗	$69.35 \pm 3.38^*$
	IW-DPO-L	✓	$\mathbf{70.50 \pm 3.46}$
	IW-DPO-R	✗	69.19 ± 3.43
	IW-DPO-R	✓	$\mathbf{72.28 \pm 4.62}$

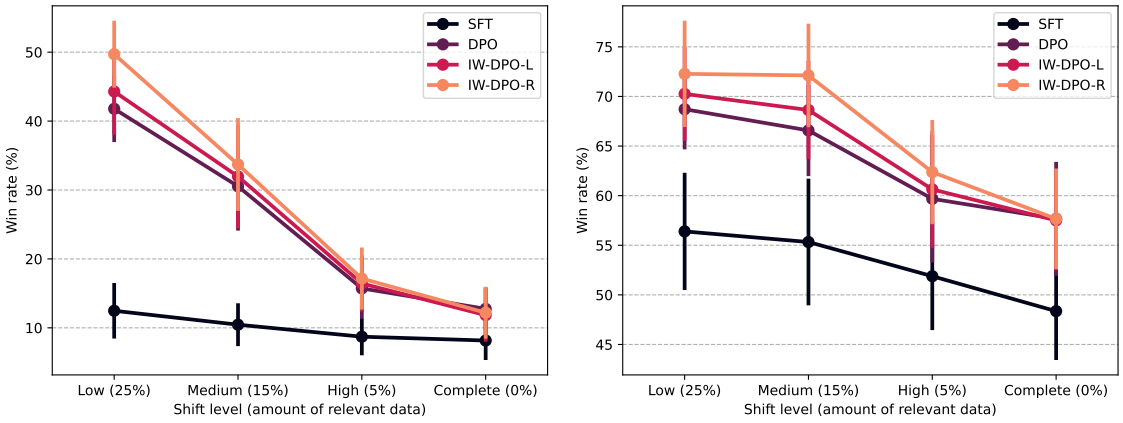

(a) Pythia-2.8B (b) Llama 3.1-8B-Instruct

Figure 5: Analysis of the win rate as a function of the amount of data from the test distribution included in the training dataset. The plots illustrate how variations in distribution shift levels impact the performance of different methods, employing Pythia-2.8B (a) and Llama 3.1-8B-Instruct (b).

sets of preferences within the training dataset. Chen et al. (2025) enhanced DPO to address its limitations in characterizing the diversity of human preferences, drawing inspiration from Mallows' theory of preference ranking to better capture the dispersion of human preferences in response to prompts. They demonstrate the robustness to out-of-distribution scenarios, but their method does not steer towards a particular distribution of interest.